

Adiabatic dynamics of a quantum critical system coupled to an environment: Scaling and kinetic equation approaches

Dario Patanè

*MATIS CNR-INFM & Dipartimento di Metodologie Fisiche e Chimiche (DMFCI),
Università di Catania, viale A. Doria 6, 95125 Catania, Italy and
Departamento de Física de Materiales, Universidad Complutense, 28040 Madrid, Spain*

Alessandro Silva

The Abdus Salam International Centre for Theoretical Physics, Strada Costiera 11, 34100 Trieste, Italy

Luigi Amico

*MATIS CNR-INFM & Dipartimento di Metodologie Fisiche e Chimiche (DMFCI),
Università di Catania, viale A. Doria 6, 95125 Catania, Italy and
Departamento de Física de Materiales, Universidad Complutense, 28040 Madrid, Spain*

Rosario Fazio

NEST-CNR-INFM & Scuola Normale Superiore, Piazza dei Cavalieri 7, I-56126 Pisa, Italy

Giuseppe E. Santoro

*International School for Advanced Studies (SISSA), Via Beirut 2 – 4, 34014 Trieste, Italy
CNR-INFM Democritos National Simulation Center, Via Beirut 2 – 4, 34014 Trieste, Italy and
The Abdus Salam International Centre for Theoretical Physics, Strada Costiera 11, 34100 Trieste, Italy*

We study the dynamics of open quantum many-body systems driven across a critical point by quenching an Hamiltonian parameter at a certain velocity. General scaling laws are derived for the density of excitations and energy produced during the quench as a function of quench velocity and bath temperature. The scaling laws and their regimes of validity are verified for the XY spin chain locally coupled to bosonic baths. A detailed derivation and analysis of the kinetic equation of the problem is presented.

I. INTRODUCTION

A series of beautiful experiments on the dynamics of cold atomic gases^{1,2,3} spurred renewed interest in the study of non-equilibrium quantum many-body systems. On the theoretical side these experiments triggered an intense investigation mostly devoted to the simplest paradigm of nonequilibrium quantum dynamics: the controlled variation in time of one of the system parameters (quantum quenches). In the case of sudden quenches, where the driving parameter is changed on a time scale much shorter than typical time scales of the system, a number of important issues have been addressed. We mention, for example, the study of the signatures of universality in the quench dynamics of quantum critical systems⁴, the presence of thermalization in integrable vs. nonintegrable systems⁵, as well as the description of generic nonequilibrium quenches using thermodynamic variables⁶ and their statistics⁷.

In this paper we will focus on the opposite case in which the control parameter is varied *adiabatically*, a case which becomes particularly interesting when a critical point is crossed during the adiabatic evolution. Because of the vanishing of the energy gap at criticality, the system is unable to follow adiabatically the driving remaining in its equilibrium/ground state when passing through the quantum critical point the system will not

be able no matter how slow is the quench. The study of these deviation from the adiabatic dynamics is a problem which is very important in a number of different branches of physics ranging from the defect formation in the early universe^{8,9} to adiabatic quantum computation¹⁰ or quantum annealing^{11,12}. Depending on the context, the loss of adiabaticity has been characterized by the excess energy at the end of the quench, by the density of defects (if the final state was a fully ordered system), or by the fidelity of the time evolved state with the ground state of the Hamiltonian at the end of the quench.

The scaling of the density of excitations generated during the dynamics as a function of the velocity of the quench was first predicted in Ref. 13, 14 for a quantum critical system. The mechanism behind the generation of excitations/defects is similar to so-called Kibble-Zurek (KZ) mechanism⁸ first proposed for classical phase transitions. Following these initial works a number of specific models were scrutinized^{15,16,17,18,19,20,21,22,23,24,25,26,27,28,29}, thereby confirming the general picture.

All the works mentioned previously assumed unitary Hamiltonian dynamics. We know, however, that understanding the effect of the external environment on the adiabatic dynamics is of paramount importance for several reasons. In the case of adiabatic quantum computa-

tion, decoherence is a fundamental limiting factor to the ability of implementing quantum algorithms. Furthermore, an experimental verification of the KZ scaling in a quantum phase transition can only occur through the detection of this effect at low temperatures, i.e. when the quantum critical system is in contact with a thermal bath. Despite its importance the adiabatic dynamics of open critical systems is a much less studied problem. The effect of classical and quantum noise acting uniformly on a quantum Ising chain was considered in Ref.30 and Ref.31 respectively. Numerical simulations for a model of local noise on a disordered Ising model were performed in Ref.32. Moreover the effect a static spin bath locally coupled to an ordered Ising model is studied in Ref.33. In a recent Letter³⁴, we have addressed the universality of the production of defects in the adiabatic dynamics in the presence of an environment by generalizing the scaling theory to open critical system and by formulating a quantum kinetic equation approach for the adiabatic dynamics across the quantum critical region. We found that, at weak coupling and for not too slow quenches the density of excitations is universal also in the presence of an external bath. In this paper we extend the results presented in Ref. 34 and provide a detailed derivation of the kinetic equations and of the scaling approach.

The paper is organized as follows. We first derive qualitatively the scaling laws obeyed by both the density of defects and of energy generated in a quench for a generic open quantum critical system (Sec.II). We then address a specific one-dimensional model possessing a quantum critical point: the XY spin chain in transverse magnetic field. To model a thermal reservoir we couple the system to a set of bosonic degrees of freedom, as in the spin-boson model. Baths are chosen with power-law spectral density and are locally coupled to strings of neighboring spins. The model, a generalization of the one studied in Ref.34, is discussed in Sec.III. For this model, we derive a kinetic equation within the Keldysh technique (Sec. IV and Appendix A1-A2) which allows us to compute the density of defects. In Sec. V (and Appendix B) we discuss the spectrum of relaxation times needed for a comparison with the scaling approach. The density of defects and of excitation generated in a quench, and a comparison with the scaling laws is presented in Sec. VI. Finally in Sec.VII we summarize our conclusions.

II. SCALING ANALYSIS

In this section we discuss the scaling laws obeyed by the density of excitations³⁴ and by the energy density following a linear quench of a control parameter h from an initial value h_i to a final one h_f , through a second-order quantum critical point at h_c . The system, during the whole dynamics, is kept in contact with a bath at temperature T . In the $h - T$ plane the adiabatic quench is described by the horizontal line shown in Fig.1. For adiabatic quenches occurring at zero temperature, the sys-

tem stops following the external drive adiabatically and can be considered as frozen around the quantum critical point. This happens roughly when the time it takes to reach and cross the quantum critical point becomes comparable to the internal time scale (the inverse gap $\Delta(h) \simeq |h - h_c|^{-\nu z}$). The determination of this crossover point is the fundamental ingredient which leads to the scaling in the case of unitary evolution^{13,14}. In the case of a finite temperature quench there is a new important timescale which enters the problem, the time at which the system enters (and eventually leaves) the quantum critical region (see Fig.1). Initially the system is in equilibrium with the bath at a low temperature ($T \ll \Delta(h_i)$) and the behavior is, to a large extent, as in the zero-temperature case. In the quantum critical region³⁵, characterized by the crossover temperature $T \sim |h - h_c|^{\nu z}$, the gap is much smaller than the temperature itself. One can therefore expect that during the interval the system spends in the quantum critical region a number of excitations will be produced by the presence of the environment. Interestingly also this contribution to the defect production obeys a scaling law³⁶.

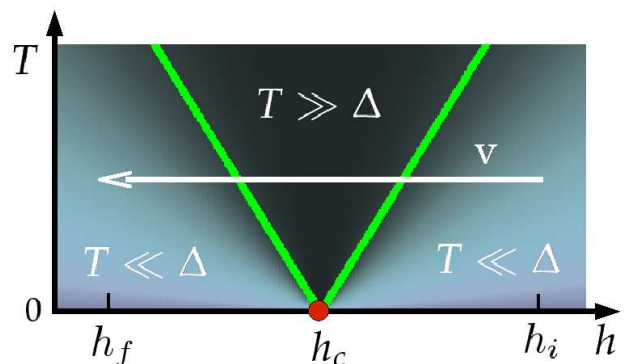


Figure 1: A sketch of the finite temperature crossover phase diagram close to the quantum critical point. Crossover lines $T \sim |h - h_c|^{\nu z}$ separating the semiclassical regions from the quantum critical region are shown. The latter is traversed by the system during the quench in a time t_{QC} .

We now proceed with the derivation of the scaling laws. In the rest of the paper we will consider the density \mathcal{E} and the energy density E of excitations, defined respectively:

$$\mathcal{E} = \int \frac{d^d k}{(2\pi)^d} \mathcal{P}_k, \quad (1)$$

$$E = \int \frac{d^d k}{(2\pi)^d} E_k \mathcal{P}_k, \quad (2)$$

where \mathcal{P}_k is the population of the excitation with quantum number k , E_k the energy spectrum at h_f , and d is the dimensionality of the quantum system.

The first assumption we make consists in separating the density of excitations/energy at the end of the quench in the sum of two (coherent and incoherent) contribu-

tions:

$$\mathcal{E} \simeq \mathcal{E}_{coh} + \mathcal{E}_{inc} , \quad (3)$$

$$E \simeq E_{coh} + E_{inc} . \quad (4)$$

In the previous equation, E_{coh} (\mathcal{E}_{coh}) is the density of energy (excitations) of the system produced coherently in the absence of the bath; the incoherent contribution E_{inc} (\mathcal{E}_{inc}) arises instead from the bath/system interaction. The separation of a coherent and an incoherent contribution, eqs. (3) and (4), requires weak coupling α between the system and the bath. Evidence for the validity of this assumption will be shown below (see Eqs.(10) and (11)).

In the absence of an environment, the density of excitations was shown to obey the KZ scaling^{13,14}

$$\mathcal{E}_{coh} = \mathcal{E}_{KZ} \propto v^{d\nu/(z\nu+1)} . \quad (5)$$

In order to obtain a similar relation for the energy density in Eq. (30) additional information on E_k at h_f is needed. Thus, the scaling of this quantity depends on the details of the system at the end of the quench. A simple scaling law can be obtained only in specific situations, e.g. for quenches halted at the critical point $h_f = h_c$, where $E_k \propto k^z$. By using techniques similar to those employed in Ref. 14 one obtains

$$E_{coh} \propto v^{\nu(d+z)/(z\nu+1)} . \quad (6)$$

Let us now derive a scaling law for the incoherent contributions \mathcal{E}_{inc} and E_{inc} . To this end it is convenient to divide the quench in three steps (see Fig. 1): initially the system is in the so-called low-temperature region at $T \ll \Delta$. Here the relatively high energy gap suppresses thermal excitation and the system remains in the ground state. Close to the critical point the system passes through the quantum critical region: thermal excitations are unavoidably created because of the relatively high temperature $T \gg \Delta$. As we shall see below, the density of excitations generated in this region are universal functions on the velocity of the quench and on the temperature as long as only the low-energy details of the system spectrum matter. On the contrary, the bath-induced relaxation occurring once the system leaves the quantum critical region, entering the other semiclassical region ($T \ll \Delta$), depends on the details of the energy spectrum; hence the relaxation towards an asymptotic thermal state at temperature T is not expected to be universal if the final h_f is far off the critical point h_c . In our analysis below we will neglect the effects of this non-universal relaxation. We are therefore assuming that the time elapsed between the moment when the critical region is left and when the quench is stopped (and the measurement of the density of excitations/energy is made) is short as compared to the typical relaxation times in the semiclassical region. In Section VI we will further comment on this point for the specific case of the quantum XY chain, showing that the scenario just depicted holds

for a wide range of h_f and v . The dynamics of the probability to excite the model k \mathcal{P}_k can be described, inside the quantum critical region, in terms of a phenomenological rate equation:

$$\frac{d}{dt}\mathcal{P}_k = -\frac{1}{\tau} [\mathcal{P}_k - \mathcal{P}_k^{th}(h_c)] , \quad (7)$$

where $\mathcal{P}_k^{th}(h_c)$ is the critical thermal equilibrium distribution and τ^{-1} is the relaxation rate, $\tau^{-1} \propto \alpha T^\theta$. As shown in Section V and appendix C, θ can be related to characteristics of the bath and to the critical indices of the phase transition (see Eq. (56)). From the relation $T \sim \Delta \sim |h - h_c|^{\nu z}$ we deduce the time spent inside the quantum critical region is

$$t_{QC} = 2T^{1/\nu z} v^{-1} .$$

A direct integration of Eq. (7) gives for the thermal excitation created in the quantum critical region $\mathcal{P}_k \sim (1 - e^{t_{QC}/\tau})\mathcal{P}_k^{th}(h_c)$. Finally, integrating the latter over all k -modes we get:

$$\mathcal{E}_{inc} \propto \left(1 - e^{t_{QC}/\tau}\right) \int dE E^{d/z-1} \mathcal{P}_k^{th}(h_c) , \quad (8)$$

where we used the scaling of the excitation energy $E \propto k^z$. For the density of energy, a similar relation holds in the case of quenches halted at the critical point

$$E_{inc} \propto \left(1 - e^{t_{QC}/(2\tau)}\right) \int dE E^{d/z} \mathcal{P}_k^{th}(h_c) , \quad (9)$$

where $t_{QC}/2$ is due to the fact that in this case only half of the quantum critical region is crossed. Finally, since the thermal distribution is a function of E/T , a simple change of variable gives the required results

$$\mathcal{E}_{inc} \propto \alpha v^{-1} T^{\theta + \frac{d\nu+1}{\nu z}} , \quad (10)$$

$$E_{inc} \propto \alpha v^{-1} T^{\theta + \frac{(d+z)\nu+1}{\nu z}} , \quad (11)$$

that are valid in the limit $T^{1/\nu z} \ll v\tau$. Eqs. (10) and (11) together with Eqs. (5) and (6) give, through the assumptions Eqs. (3) and (4), the general scaling-law for the quench dynamics of open systems. The different scaling of the two contributions with respect to the velocity v implies that for slow quenches $v < v_{cross}$ the incoherent mechanism of excitation dominates over the coherent one, and viceversa for $v > v_{cross}$. The crossover velocity can be deduced by equating $\mathcal{E}_{inc} \simeq \mathcal{E}_{coh}$ and $E_{inc} \simeq E_{coh}$ yielding:

$$v_{cross}^{\mathcal{E}} \propto \alpha^{\frac{\nu z+1}{\nu(z+d)+1}} T^{\left(1 + \frac{(\theta-1)\nu z}{\nu(z+d)+1}\right)\left(1 + \frac{1}{\nu z}\right)} , \quad (12)$$

$$v_{cross}^E \propto \alpha^{\frac{\nu z+1}{\nu(2z+d)+1}} T^{\left(1 + \frac{(\theta-1)\nu z}{\nu(2z+d)+1}\right)\left(1 + \frac{1}{\nu z}\right)} . \quad (13)$$

III. QUANTUM XY MODEL WITH THERMAL RESERVOIR

The scaling laws derived above will be tested against a specific model: an XY-chain coupled to a set of bosonic

baths. The Hamiltonian of the XY chain is defined as

$$H_S = -\frac{1}{2} \sum_j^N \left(\frac{1+\gamma}{2} \sigma_j^x \sigma_{j+1}^x + \frac{1-\gamma}{2} \sigma_j^y \sigma_{j+1}^y + h \sigma_j^z \right). \quad (14)$$

Here N is the number of sites (σ^x, y, z are Pauli matrices). Each spin is coupled to its neighbors by anisotropic Ising-like interaction and subject to a transverse magnetic field h (the couplings are expressed in terms of the exchange energy). In the thermodynamic limit $N \rightarrow \infty$, a quantum phase transition at $h_c = 1$ separates a paramagnetic phase for $h > 1$ from a ferromagnetic phase ($h < 1$) where the Z_2 symmetry is spontaneously broken and a magnetic order along \vec{x} appears, $\langle \sigma^x \rangle \neq 0$.

The spin Hamiltonian Eq. (14) can be diagonalized by using the Jordan-Wigner transformation³⁷ to map the spins into spinless fermions c_j and thus obtain in momentum space (after a projection in a definite parity subspace)

$$H_S = \sum_{k>0} \Psi_k^\dagger \hat{\mathcal{H}}_k \Psi_k$$

$$\hat{\mathcal{H}}_k = -(\cos k + h) \hat{\tau}_z + \gamma \sin k \hat{\tau}_y, \quad (15)$$

where $\Psi_k^\dagger = (c_k^\dagger, c_{-k})$ are Nambu spinors and $\hat{\tau}$ are Pauli matrices in Nambu space. Finally, a Bogoliubov rotation diagonalizes the Hamiltonian: $H_S = \sum_{k>0} \Lambda_k (\eta_k^\dagger \eta_k - \eta_{-k}^\dagger \eta_{-k})$, where

$$\Lambda_k = \sqrt{(\cos k + h)^2 + (\gamma \sin k)^2}, \quad (16)$$

is the quasi-particle dispersion. At $h = h_c$ the spectrum becomes gapless with a linear dispersion relation $\Lambda_k \propto \pi - k$; accordingly, the critical indexes of the model are $\nu = z = 1$.

The spins are also locally coupled to a set of N/l bosonic baths

$$H_{int} = -\frac{1}{2} \sum_{j=0}^{N/l-1} \left(\sum_{r=0}^{l-1} \sigma_{jl+r}^z \right) X_j \quad (17)$$

where $X_j = \sum_\beta \lambda_\beta (b_{\beta,j}^\dagger + b_{-\beta,j})$ and $b_{\beta,j}^\dagger$ ($b_{\beta,j}$) are the creation (annihilation) operators of the j -th bosonic bath. As a result of the coupling in Eq. (17) each bath is correlated in a string of l adjacent spins. The model presented above generalizes the one considered in Ref. 34, where the spins were individually coupled ($l = 1$) to Ohmic baths ($s = 1$).

The total Hamiltonian reads:

$$H = H_S + H_{int} + H_B \quad (18)$$

where $H_B = \sum_{j,\beta} \omega_\beta b_{\beta,j}^\dagger b_{\beta,j}$. The spectral density of the baths $J(\omega) = \sum_\beta \lambda_\beta^2 \delta(\omega - \omega_\beta)$ is

$$J(\omega) = 2\alpha \omega^s e^{-\omega/\omega_c} \theta(\omega) \quad (19)$$

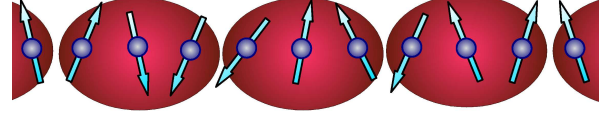


Figure 2: A cartoon of the spins-baths coupling (17) for the $l = 3$, where each bath is coupled to three spins.

where α is the system/bath coupling, ω_c is a high energy cutoff and $\theta(s)$ is the step function³⁸.

In the situation we are interested, the system is initialized in its ground state at large h . The coupling of the spin to the bath through σ^z preserves parity symmetry (see Eq. (20)). Therefore, once the system has initially a specific parity, it will remain in the corresponding sector for the entire evolution. Throughout this paper we consider N even: in this case the ground state has always an even number of fermions c_k and we are thus allowed to select the even parity sector and neglect the odd one.

In momentum space $b_{\beta,q} = \frac{1}{\sqrt{N/l}} \sum_{j=0}^{N/l-1} \exp(-iqj) b_{\beta,j}$ with $q = \frac{2m\pi}{N/l}$ and after the Jordan-Wigner transformation we get

$$H_{int} = -\frac{1}{\sqrt{N}} \sum_k \sum_q F(q) \Psi_k^\dagger \hat{\tau}^z \Psi_{k+q} X_q \quad (20)$$

where $F(q) = 1/\sqrt{l} \sum_{r=0}^{l-1} \exp(-irq/l)$. For $l = 1$ each spin interact with a different bath and according to Eq. (20) all k modes are coupled (i.e., transitions $k \leftrightarrow k'$, $\forall k, k'$ are induced). In the opposite case of $l = N$ (just one bath for the whole system) no transition between different k is allowed. In the intermediate case each mode interacts with the other modes in an interval of width $2\pi l/N$.

It is important to notice that correlations between baths over a finite distance would not change qualitatively our picture as long as we focus on the critical properties of the model. Indeed, near criticality the divergence of the correlation length makes the details of the bath correlations over microscopic distances unimportant. For the same reason, as long as one is interested in the low- T properties of the bath, the specific value of l is not relevant provided $l/N \rightarrow 0$ in the thermodynamic limit. Specifically, for all values of l such that $T \ll (\frac{1}{l})^z$ the same dissipative dynamics is obtained, since transitions with large Δk (and hence large energy) are thermally suppressed (we used $E \propto k^z$ at a fixed T). In this regime, therefore, the system cannot resolve the microscopic details of different system-bath couplings (i.e., whether $l = 1, 2, 3, \dots$). In the following, we thus focus on the case $l = 1$: specific high-temperature and non-critical behaviors for different l could be easily investigated within the same scheme considered below. Only if $l = N$ the dynamics of the system changes qualitatively.

IV. KINETIC EQUATION

In this section we derive a kinetic equation for the Green's function of the Jordan-Wigner fermions within the Keldysh formalism. In terms of this Green's function we will then calculate both the excitation and the energy densities, Eq. (1) and (2). Our analysis in terms of a kinetic equation will provide support for the scaling laws obtained above, Eqs. (10)-(11), while allowing us to study the non-universal dynamics beyond the limit of applicability of the scaling approach.

The fermionic Keldysh Green's function is a matrix in Nambu space defined by

$$[G_k(t_1, t_2)]_{i,j} \equiv -i \langle \mathcal{T}_\gamma \Psi_{ki}(t_1) \Psi_{kj}^\dagger(t_2) \rangle \quad (21)$$

(see appendix A1 for notations) where γ is the Keldysh contour. In the following we will neglect the initial correlations between system and bath⁴¹. Hence γ consists of just a forward and backward branch on the real time axis. Below we will sketch of the main steps of the derivation: the remaining details can be found in Appendix A1-A2.

The starting point of our derivation is the Dyson's equation in its integro-differential form

$$\begin{aligned} [i\partial_{t_1} - \hat{\mathcal{H}}_k(t_1)] G_k(t_1, t_2) &= \delta(t_1 - t_2) \\ &+ \int_\gamma d\bar{t} \Sigma_k(t_1, \bar{t}) G_k(\bar{t}, t_2) \end{aligned} \quad (22)$$

and an analogous one obtained by differentiation with respect t_2 . Here Σ_k is the self-energy associated to the interaction of the system with the bath. In order to compute the energy and excitations density we need to find the equal-time statistical Green's functions. The latter are defined as

$$[G_k^<(t_1, t_2)]_{i,j} \doteq i \langle \Psi_{k,j}^\dagger(t_2) \Psi_{k,i}(t_1) \rangle \quad (23)$$

$$[G_k^>(t_1, t_2)]_{i,j} \doteq -i \langle \Psi_{k,i}(t_1) \Psi_{k,j}^\dagger(t_2) \rangle \quad (24)$$

An equation for these correlators can be obtained from Eq. (22) by using standard techniques⁴⁰ (see Appendix A1 for details). For the equal-time Green's function $G_k^<(t, t)$ we obtain:

$$\begin{aligned} i\partial_t G_k^< &= [\hat{\mathcal{H}}_k, G_k^<] + \\ &\Sigma_k^> \cdot G_k^< - \Sigma_k^< \cdot G_k^> + G_k^< \cdot \Sigma_k^> - G_k^> \cdot \Sigma_k^<, \end{aligned} \quad (25)$$

where the dots indicate the convolution:

$$\Sigma_k^> \cdot G_k^< \doteq \int_0^t d\bar{t} \Sigma_k^>(t, \bar{t}) G_k^<(\bar{t}, t).$$

In order to proceed with the solution of Eq. (25) it is now important to discuss the approximations we make for the self-energy. Let us first notice that long-time correlations induced by the bath may change the universality class of the transition, by renormalizing the low energy

spectrum of the system³⁹. As previously mentioned, we will not consider this case here. Therefore, we assume that the bosons have a non-zero inverse lifetime $\Gamma \ll T$ which provides a natural cutoff-time for the bath correlation functions. Within this assumption it is now possible to describe the kinetics of the system using a Markov approximation together with a self-consistent Born approximation. The latter is justified for weak system/bath coupling ($\alpha \ll 1$) and is represented diagrammatically in Fig. 3-(a). We will neglect the tadpole diagram (b),

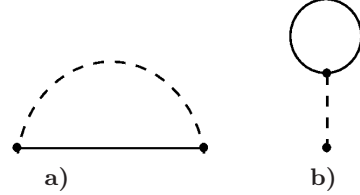


Figure 3: Lowest-order diagrams contributing to the self-consistent Born approximation: dashed lines correspond to the non-interacting bath Green's function g , while solid lines to the interacting system Green's function G . **a)** corresponds to Eq. (46), while **b)** to Eq. (47).

which represents just a small shift of the energy levels.

By going to the interaction picture

$$\tilde{G}_k(t_1, t_2) \doteq \hat{\mathcal{U}}_k^\dagger(t_1) G_k(t_1, t_2) \hat{\mathcal{U}}_k(t_2),$$

it is now evident that, within our assumptions, the evolution of \tilde{G}_k can be considered slow as compared to that of the bath correlators appearing in the self-energies. Using this separation of time scales it is possible to implement the Markov approximation and transform the general integro-differential kinetic equation into a simple differential equation (see Appendix A1-A2). We then obtain, in the case in which each spin is coupled to its own bath ($l = 1$), the kinetic equation

$$\partial_t G_k^< + i [\mathcal{H}_k, G_k^<] = \quad (26)$$

$$\frac{1}{N} \sum_q \tau^z (\mathbf{1} + iG_q^<) \hat{D}_{qk} G_k^< + \tau^z G_q^< \hat{D}_{kq}^\dagger (\mathbf{1} + iG_k^<) + H.c.$$

where

$$\hat{D}_{qk} = i \int_0^\infty ds g^>(s) \hat{\mathcal{U}}_q^\dagger(t, t-s) \hat{\tau}^z \hat{\mathcal{U}}_k(t, t-s), \quad (27)$$

$g^>(t) = -i \langle X_q(t) X_q(0) \rangle$, and $\hat{\mathcal{U}}_k(t_0, t)$ is the evolution operator satisfying $i\partial_t \hat{\mathcal{U}}_k = \hat{\mathcal{H}}_k(t) \hat{\mathcal{U}}_k$. The left-hand-side of Eq. (26) represents the free evolution term, while the right-hand-side describes the scattering between the k modes mediated by the bath degrees of freedom. Notice that the number of equations scales linearly with the system size N , in contrast to conventional systems of master equations whose number scales exponentially with N as a result of the fact that the full density matrix (i.e. all m -points Green's functions) is considered. The fact that

we are considering only the two-point Green's function self consistently using the Born approximation is responsible for the non-linear nature of Eq. (26), in contrast to the linearity of the master equation.

In the eigenbasis of the Hamiltonian $\hat{\mathcal{H}}_k$ the Green's function can be parameterized as

$$-iG_k^< = \begin{pmatrix} \mathcal{P}_k & \mathcal{C}_k \\ \mathcal{C}_k^* & 1 - \mathcal{P}_k \end{pmatrix} \quad (28)$$

where $\mathcal{P}_k = \langle \eta_k^\dagger \eta_k \rangle$ is the population of the excited mode k and $\mathcal{C}_k = \langle \eta_{-k} \eta_k \rangle$ can be regarded as a ‘‘coherence’’ term⁴⁴. In the static case, where the evolution operator is $\hat{\mathcal{U}}_k = \exp(-i\hat{\mathcal{H}}_k t)$, the stationary solution of the kinetic equation (26) is correctly the thermal equilibrium one: $\mathcal{C}_k = \mathcal{C}_k^{th} = 0$ and $\mathcal{P}_k = \mathcal{P}_k^{th} = (e^{\Lambda_k/k_B T} + 1)^{-1}$ (the Fermi function).

Finally, once the solution of the kinetic equation (26) is obtained, the density of excitations and energy produced during the quench can be expressed as

$$\mathcal{E} = \frac{1}{N} \sum_{k>0} \mathcal{P}_k \quad (29)$$

$$E = \frac{1}{N} \sum_{k>0} \Lambda_k \mathcal{P}_k \quad (30)$$

We conclude this section by commenting on a useful approximation to evaluate numerically the kernel of \hat{D}_{qk} , Eq. (27), discussed in full detail in Appendix A2. It consists in approximating the evolution operator $\hat{\mathcal{U}}_k$ appearing in \hat{D}_{qk} with $\hat{\mathcal{U}}_k(t, t-s) \simeq \exp(i\hat{\mathcal{H}}_k(t)s)$, thus obtaining

$$\hat{D}_{qk} \simeq i \int_0^\infty ds g^>(s) \exp(-i\hat{\mathcal{H}}_k(t)s) \hat{\tau}^z \exp(i\hat{\mathcal{H}}_k(t)s). \quad (31)$$

This is again consistent with the separation of time scales mentioned above, and in particular with the Markov ap-

proximation. Indeed, while the exact relaxation rate matrix (27) depends on the velocity of the quench, if the quench is slow on the time scale characteristic of the bath, the correlation function $g^>(s)$ can be seen as strongly peaked at $s = 0$. Hence the system can be considered ‘‘frozen’’ at the instantaneous value of $h(t)$ and, consistently, its evolution operator is the exponential of the Hamiltonian.

V. RELAXATION TIME

In order to make further progress in understanding the quench dynamics of the system we will first extract from the kinetic equation the characteristic relaxation time for the populations of the excitations \mathcal{P}_k (see Eq.(28)) as a function of the magnetic field h and the temperature T . For this purpose, it is sufficient to consider only the diagonal elements of Eq. (28). This is equivalent to the so called ‘‘secular approximation’’ for the master equation⁴⁴, which is valid for weak couplings ($\alpha \ll 1$ in the present case). For generic N , we deal with a set of $N/2$ equations (only $N/2$ modes are independent) of the form:

$$\frac{d}{dt} \mathcal{P}_k = a_k + \sum_q b_{kq} \mathcal{P}_q + \sum_q c_{kq} \mathcal{P}_k \mathcal{P}_q.$$

The asymptotic relaxation can be studied by linearizing the previous set of equations near the thermal equilibrium fixed point. We obtain, with the vector notation $\delta \underline{\mathcal{P}} = (\delta \mathcal{P}_1, \delta \mathcal{P}_2, \dots, \delta \mathcal{P}_{N/2})^{\text{tr}}$ where $\delta \mathcal{P}_k = \mathcal{P}_k - \mathcal{P}_k^{th}$:

$$\frac{d}{dt} \delta \underline{\mathcal{P}} = -\mathcal{R} \delta \underline{\mathcal{P}} \quad (32)$$

where non-linear terms in $\delta \mathcal{P}_k$ have been neglected. The diagonal and off-diagonal elements of the $N/2 \times N/2$ matrix \mathcal{R} are:

$$\begin{aligned} \mathcal{R}_{kk} = & \frac{2}{N} \sum_{q>0, q \neq k} [\mathcal{G}_q^{th} (1 - \cos(\theta_k + \theta_q)) g[-\Lambda_k - \Lambda_q] + \mathcal{G}_q^{th} (1 + \cos(\theta_k + \theta_q)) g[\Lambda_k - \Lambda_q] \\ & + \mathcal{P}_q^{th} (1 - \cos(\theta_k + \theta_q)) g[\Lambda_k + \Lambda_q] + \mathcal{P}_q^{th} (1 + \cos(\theta_k + \theta_q)) g[-\Lambda_k + \Lambda_q]] \\ & + \frac{2}{N} 4 \sin^2 \theta_k (\mathcal{G}_k^{th} g[-2\Lambda_k] + \mathcal{P}_k^{th} g[2\Lambda_k]) \end{aligned} \quad (33)$$

$$\begin{aligned} \mathcal{R}_{kq} = & \frac{2}{N} [-\mathcal{G}_k^{th} (1 + \cos(\theta_k + \theta_q)) g[-\Lambda_k + \Lambda_q] + \mathcal{G}_q^{th} (1 - \cos(\theta_k + \theta_q)) g[-\Lambda_k - \Lambda_q] \\ & - \mathcal{P}_q^{th} (1 + \cos(\theta_k + \theta_q)) g[\Lambda_k - \Lambda_q] + \mathcal{P}_q^{th} (1 - \cos(\theta_k + \theta_q)) g[\Lambda_k + \Lambda_q]] \end{aligned} \quad (34)$$

where $g[E]$ is the Laplace transform of bath correlator (50), \mathcal{G}_k^{th} is the thermal equilibrium value of the pop-

ulation of the ground-state of mode k , $\mathcal{G}_k^{th} = 1 - \mathcal{P}_k^{th}$,

and

$$\theta_k = \arccos -\frac{(\cos k + h)}{\Lambda_k}. \quad (35)$$

The eigenvalues of \mathcal{R} , $\{\lambda_i\}$, are the characteristic relaxation rates of the long-time dynamics. Hence the solution of Eq. (32) for each population would be a linear combination containing all the characteristic relaxation times:

$$\delta\mathcal{P}_k = \sum_j r_{kj} e^{-\lambda_j t}$$

At long times $t \gg (\min_j \lambda_j)^{-1} \doteq \tau$ all modes relax with the same relaxation time τ . In the following we first analyze the longest relaxation time τ , extending the results presented in Ref. 34; we then study the structure of the entire spectrum of relaxation times.

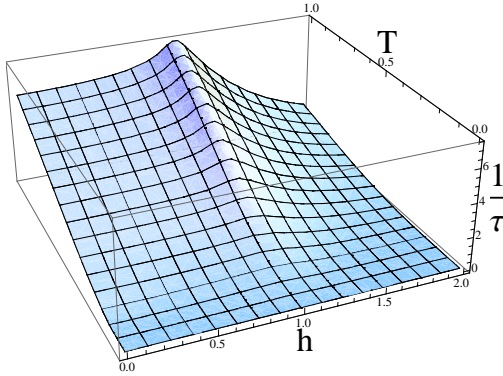


Figure 4: Relaxation rate $1/\tau$ as a function of T and h for $N = 400$ (here $\gamma = 1$, and $s = 1$).

In Fig. 4 we show the general behavior of τ in the finite temperature phase-diagram, calculated by numerically diagonalizing the matrix \mathcal{R} . As $T \rightarrow 0$, τ diverges and close to the critical point two different behaviors are found in the semiclassical regions and in the quantum critical region (see also Fig.1):

$$\tau^{-1} \propto \begin{cases} T^{1+s} & T \gg \Delta \\ e^{-\Delta/T} & T \ll \Delta \end{cases} \quad (36)$$

These relations extend the results obtained for the relaxation rate in Ref. 34 to the generic case of non-Ohmic baths and give the exponent θ as $\theta = 1 + s$.

An analytic expression for the power-law scaling inside the quantum critical region can be obtained by approximating the smallest eigenvalue of \mathcal{R} with the smallest diagonal element. This is justified by the fact that the off-diagonal elements are of the order $O(1/N)$ (see Eq. (34)). For $h = h_c = 1$, considering the gapless mode $k = \pi$, we

have from Eq. (33) in the continuum limit:

$$\begin{aligned} \tau_{diag}^{-1} &\doteq \mathcal{R}_{\pi\pi} = \frac{2}{\pi} \int_0^\pi dq (\mathcal{G}_q^{th} g[-\Lambda_q] + \mathcal{P}_q^{th} g[\Lambda_q]) \\ &= 4\alpha \int_0^\pi dq \frac{\Lambda_q^s}{\sinh(\Lambda_q/T)} \\ &\simeq 8\alpha (1 - 2^{-1-s}) \Gamma(1+s) \zeta(1+s) (\gamma/T)^{-1-s} \end{aligned} \quad (37)$$

where Γ and ζ are the Gamma and the zeta functions, and we used the critical dispersion relation $\Lambda_q \simeq \gamma(\pi - q)$ obtained by linearizing Eq. (16) around the gapless point $k = \pi$ (we extended the integration to $-\infty$ since at low-temperature only the low-energy modes contribute to the integral). Fig. 5 demonstrates that the analytical expression in Eq. (37) agrees very well with the numerical solution (obtained by diagonalizing \mathcal{R}), especially at low temperature.

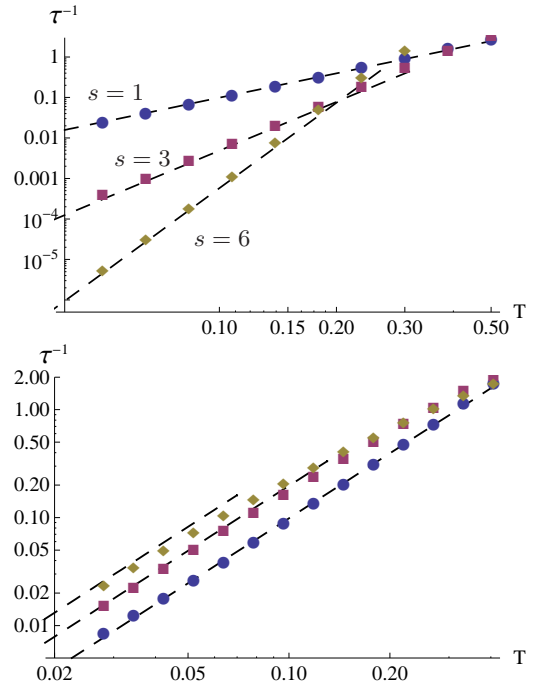


Figure 5: Relaxation rate $1/\tau$ as a function of T as obtained from the exact diagonalization of \mathcal{R} (symbols) and the approximation in Eq. (37) (dashed lines). Upper panel: $s = 1, 3, 6$, with $\gamma = 1$; lower panel: $s = 1$ with different $\gamma = 0.3, 0.5, 1$ from top to bottom.

As we have shown in Fig. 5, inside the quantum critical region the exponent θ is universal within the range of anisotropy $0 < \gamma \leq 1$ where the system belongs to the Ising universality class. This suggests a relation between θ and the critical indexes of the quantum phase transition. Indeed, it can be shown, within the Fermi golden rule (see Appendix B), that for a generic system coupled to a bosonic bath the following expression holds inside the quantum critical region:

$$\tau^{-1} \propto T^{s+d/z}. \quad (38)$$

An important feature of the relaxation dynamics can be extracted by analyzing the spectrum of the eigenvalues $\{\lambda_j\}$ of \mathcal{R} . In Fig. 6 the λ_j 's are shown for some values of temperature and magnetic field. We find that in the semiclassical regions $T \ll \Delta$ the smallest eigenvalue of \mathcal{R} is separated from the rest of the spectrum by a gap (even in the $N \rightarrow \infty$ limit). On the contrary, inside the quantum critical region such eigenvalue merges with the rest of the spectrum. This can be quantified by the relative gap of the spectrum of relaxation times, that is identified by $(\lambda_2^{-1} - \lambda_1^{-1})/\lambda_1^{-1}$, being $\lambda_{1,2}$ the lowest eigenvalues of \mathcal{R} (see Fig. V). Such result indicates that while the exponential divergence of the relaxation time $\tau \propto \exp\{\Delta/T\}$ in the semiclassical regions is due to an isolated eigenvalue, the long-time behavior in the quantum critical region is, instead, built up by a continuum of eigenvalues contributing to the $\tau^{-1} \propto T^2$ scaling.

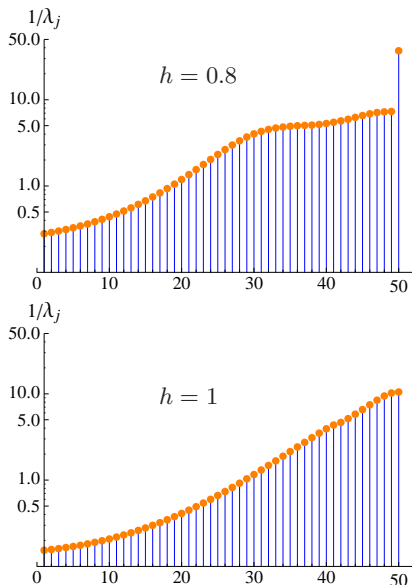


Figure 6: Spectrum of the eigenvalues of \mathcal{R} for the Ising model ($\gamma = 1$) with Ohmic baths ($s = 1$), for $N = 100$. The values of temperature $T = 0.1$ and magnetic field $h = 0.8$, or 1 are chosen to belong, respectively, to the semiclassical and the quantum critical region.

VI. ADIABATIC QUENCHES

Equipped with the kinetic equation and the knowledge of the scaling of the relaxation times, we now analyze the quench dynamics of the model in Eq. (18)) by solving the kinetic equation (26) numerically. The system is initialized at $h_i \gg h_c$ in equilibrium with the bath at a fixed temperature $T \ll \Delta(h_i)$, and the transverse field is then ramped linearly $h(t) = h_i - vt$ down to a final value h_f (the bath temperature is kept fixed).

In Fig. 8 we plot the density of excitations as a function of the quench velocity for different system sizes (a

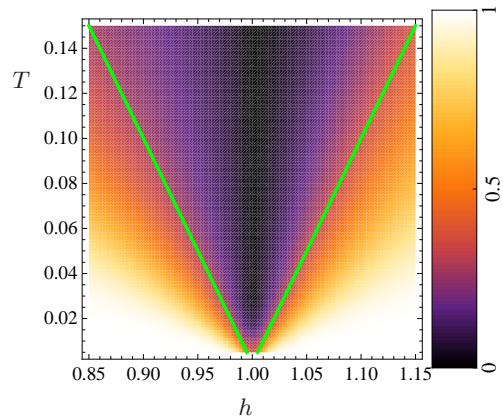


Figure 7: Ising model ($\gamma = 1$) with Ohmic baths ($s = 1$). Relative gap between the two longest relaxation times: $(\lambda_2^{-1} - \lambda_1^{-1})/\lambda_1^{-1}$ ($\lambda_{1,2}$ being the two lowest eigenvalue of \mathcal{R}); crossover lines $T = T_{cross} = |h - 1|$ are plotted for comparison.

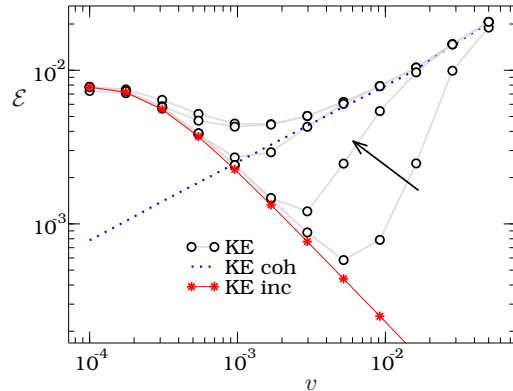


Figure 8: Density of excitation \mathcal{E} (circles) Vs quench velocity for different system sizes $N = 26, 50, 100, 200, 400, 800$ from bottom to top, according to the arrow; the points corresponding to $N = 800$ and $N = 400$ are indistinguishable. Parameters are set $\alpha = 0.01$, $T = 0.1$, $\gamma = 1$ and $s = 1$ and the quench is halted at $h_f = 0.8$. Dotted line is the coherent contribution \mathcal{E}_{coh} obtained for $\alpha = 0$ and stars represent the incoherent contribution \mathcal{E}_{inc} due to thermal excitation (see text); both curves refer to $N = 800$, even if for \mathcal{E}_{inc} the same curve is obtained already at $N \sim 30$.

similar behavior is obtained for the density of energy). Additionally we considered separately the coherent (\mathcal{E}_{coh}) and incoherent contribution (\mathcal{E}_{inc}) to the final density of excitations. The first one is obtained by integrating the kinetic equation for $\alpha = 0$, i.e. no coupling with the bath. The incoherent term is due to thermal excitations created by the bath and it is obtained by integrating the kinetic equation and ignoring the unitary evolution term $i[\hat{\mathcal{H}}_k, \hat{G}_k^<]$, responsible for the coherent excitation process.

In order to understand the two excitation mechanisms we analyse directly the dynamics of the populations \mathcal{P}_k . From the results shown in Fig 9 (left) it emerges that excitations are generated close to the critical point and when the system is driven in the semiclassical region (and

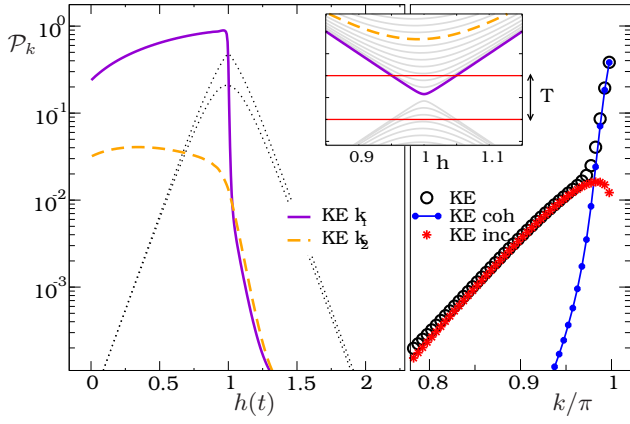


Figure 9: Populations of the excited states \mathcal{P}_k for $N = 400$, $v = 0.0017$ and the same values of Fig. 8. Left: dynamics of two low energy modes $k_1 \sim \pi$ (dashed line) and $k_2 \sim 0.9\pi$ (dotted-dashed line) obtained by solving the kinetic equation (instantaneous thermal equilibrium values are plotted as reference as dotted lines). The Inset shows the energy levels near the critical point and the scale of temperature; marked levels of the excited band refer to k_1 and k_2 . The energy gap closes at $k = \pi$. Right: distribution of \mathcal{P}_k as a function of the mode k at $h(t) = 1$. Stars represent the excitations created incoherently and triangles are the coherent excitations produced in the case of no coupling to the bath. The two excitation mechanisms act on different energy scales, being lowest energy modes coherently populated and the highest one thermally excited.

$T \ll \Delta$) they are relaxed out by the bath. The density of excitation generated is the sum of the the incoherent and coherent contribution, thus proving the validity of the *Ansatz* (3) and (4) (see Fig. 9 (right)).

For the XY model the integration of Eqs. (8) and (9) can be performed explicitly by using the critical spectrum $\Lambda_k \sim \gamma(\pi - k)$. We obtain:

$$\mathcal{E}_{inc} = \frac{\log 2}{2\pi\gamma} T \left(1 - e^{-2T/(\tau v)}\right) \quad (39)$$

$$E_{inc} = \frac{\pi}{24\gamma} T^2 \left(1 - e^{-T/(\tau v)}\right) \quad (40)$$

where the latter holds for quenches halted at $h_f = h_c$. In the previous formulas, the expression derived for τ in Eq. (37) can be used to get a fully analytical expression. Expanding the exponentials in Eqs. (39) and (40) we obtain

$$\mathcal{E}_{inc} \simeq \frac{8 \log 2}{\pi} \varphi(s) \alpha \gamma^{-2-s} v^{-1} T^{3+s} \quad (41)$$

$$E_{inc} \simeq \frac{\pi}{3} \varphi(s) \alpha \gamma^{-2-s} v^{-1} T^{4+s} \quad (42)$$

where $\varphi(s) = (1 - 2^{-1-s})\Gamma(1+s)\zeta(1+s)$. The previous relations are consistent with Eqs.(10) and (11) with $\theta = 1 + s$ (see Eq. (38)).

In Fig. 10 the density of excitations and energy obtained from the solution of kinetic equation is compared with the scaling-law derived in Sec. II using the specific

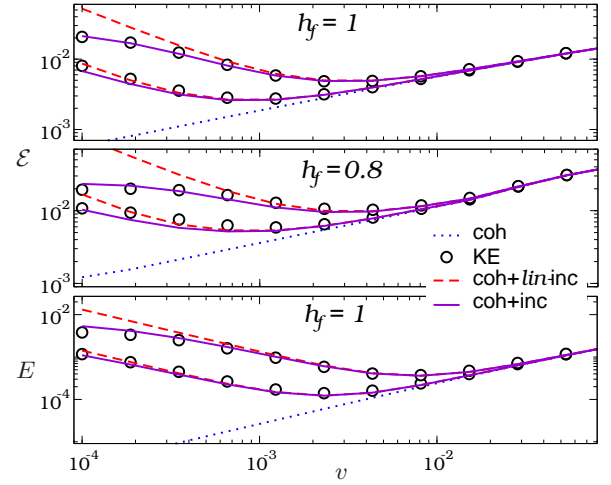


Figure 10: Density of energy (lowest panel) and of excitations versus quench velocity v for $h_f = 0.8$, and 1. Parameters are set to $\gamma = 0.7$, $s = 1.5$, $\alpha = 0.01$, and $T = 0.15$, or 0.1 (upper and lower curves of each panel). Circles are obtained by solving the kinetic equation; dotted lines are the coherent contributions \mathcal{E}_{coh} and E_{coh} evaluated by solving the kinetic equation for $\alpha = 0$; a fit gives correctly $\mathcal{E}_{coh} \propto \sqrt{v}$ and $E_{coh} \propto v$ consistently with the KZ scaling-law for excitations (5) and the modified scaling we derived for the energy density (6). Solid and dashed lines are Eqs. (3) and (4) using for the incoherent contributions the expressions (39) and (40) and their linearized forms (41) and (42), respectively.

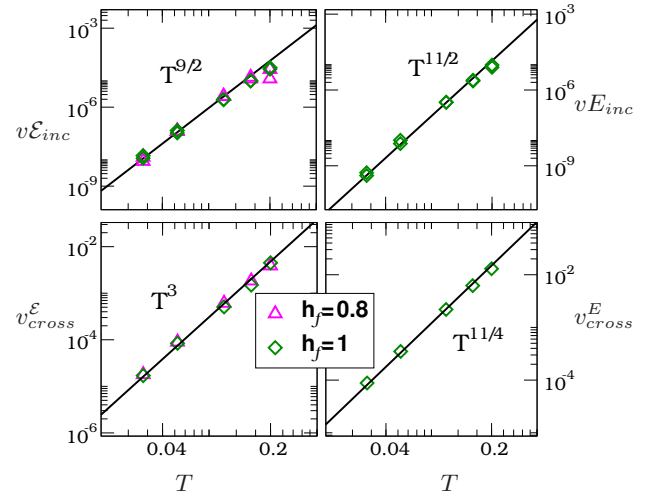


Figure 11: System and bath parameters are fixed as in of Fig. 10. Upper panel: Data collapse of \mathcal{E}_{inc} and E_{inc} obtained from the kinetic equation; data refer to $10^{-3} \lesssim v \lesssim 10^{-2}$ (data relative to $h_f = 1$ for \mathcal{E}_{inc} are rescaled by a factor 2, since in this case only half quantum critical region is crossed). Lower panel: scaling of v_{cross} is obtained equating $\mathcal{E}_{inc} = \mathcal{E}_{coh}$ and analogously for E . The fits confirm the scaling predicted by (10), (11) and (12), (13), that, for the specific case of $s = 1.5$ considered, are shown in their corresponding plots.

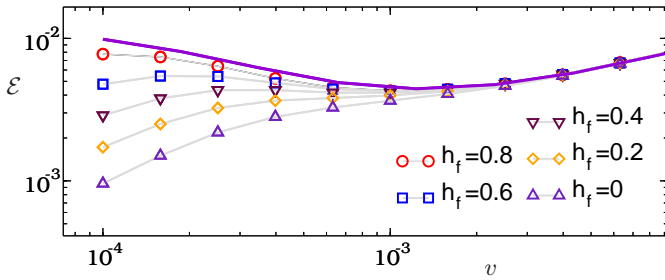


Figure 12: Density of excitations versus quench velocity v for $h_f = 0.8, 0.6, 0.2, 0$. Parameters are set to $\gamma = 1$, $s = 1$, $\alpha = 0.01$ and $T = 0.1$. Upper solid line is the scaling-law (3) using the expression (39). Decreasing the value of h_f , the crossing of the semiclassical region, after the critical point, becomes more relevant at low v and scaling no longer holds strictly.

expressions, Eqs. (39) and (40), derived above for the XY model. The scaling-laws are found in good agreement with the numerical data. The results shown in Fig. 11 further confirm the scaling as a function of the temperature and the relations (12), (13) for the crossover velocity.

Finally we comment on the role of the final value of magnetic field h_f at which the quench is halted. The agreement with the scaling *Ansatz* becomes worse for decreasing h_f (see Fig. 12). This is due to the non-critical relaxation induced by the bath when the system crosses the semiclassical region after the critical point (see Fig. 1 and Fig. 9 left). At low v the time spent therein at a relative low-temperature $T \ll \Delta$ is so long that the bath is able to relax the excitations created close to the critical point.

VII. CONCLUSIONS

We have studied the dynamics of a quantum critical system coupled to a thermal reservoir and subject to an adiabatic quench across its quantum critical point. We considered the regime of weak coupling, low-temperature and slow quench velocity.

The bath has two effects on the system: the first one is to create excitations inside the quantum critical region and the second one is to trigger the relaxation of the excitations created close to the critical point when the system is driven in the semiclassical region (see Fig. 1). While the first mechanism is universal, being entirely ruled by the critical properties of the low-energy spectrum, the latter depends on the details of the system far-off the critical point. Hence, as far as the evolution is halted close to the critical point and the non-critical relaxation mechanism is negligible, universal scaling behavior is recovered. We derived scaling-laws for the density of energy produced by the quench at finite temperature extending the previous results obtained for the density of excitations in Ref. 34.

To check the validity of the scaling-laws, we considered the specific case of the quantum XY model (14) coupled locally to a set of bosonic baths, Eq. (17) (see Fig. 2). In order to study the dynamics we derived a kinetic equation, within the Keldysh formalism. A detailed analysis of the characteristic relaxation time obtained from the kinetic equation was given in Sec. V. An analytic expression for the critical relaxation time was obtained in Eq. (37) and verified in Fig. 5. As shown in Appendix B, the scaling of the latter as a function of the temperature is related to the critical exponents of the model (see Eq. (56)). Finally, we considered the quench dynamics. The kinetic equations derived allow us to study the dissipative dynamics also beyond the universal regime. We checked the scaling-laws derived and their range of validity in Figs. 10 and 12.

We remark that the method described here to obtain a kinetic equation for the XY model, may be extended to describe the dissipative dynamics of other models that can be mapped into fermionic degrees of freedom, like other spin chains and ladders or certain $2d$ models of the Kitaev-type.

Acknowledgments

We acknowledge F. Guinea, V. Kravtsov, A. Polkovnikov, A.J. Leggett, R. Raimondi and F. Sols, T. Caneva, G. Carleo and M. Schirò for fruitful discussions. D.P. acknowledges the ISTANS (grant 1758) program of ESF for financial support.

APPENDIX A1: KINETIC EQUATION

Here we present a detailed derivation of the kinetic equation. Apart from the Keldysh (21), lesser (23) and greater (24) Green's function we need also the retarded and the advanced ones, and also the bath Green functions:

$$\begin{aligned} G_{kij}^{a(r)}(t_1, t_2) &\doteq (-)i\theta(t_{2(1)} - t_{1(2)}) \left\langle \left\{ \Psi_{ki}(t_1), \Psi_{kj}^\dagger(t_2) \right\} \right\rangle \\ g_q(t_1, t_2) &\doteq -i \langle \mathcal{T}_\gamma X_q(t_1) X_q(t_2) \rangle \\ g_q^{(< >)}(t_1, t_2) &\doteq (-)i \langle X_q(t_{2(1)}) X_q(t_{1(2)}) \rangle \\ g_q^{a(r)}(t_1, t_2) &\doteq (-)i\theta(t_{2(1)} - t_{1(2)}) \langle [X_q(t_1), X_q(t_2)] \rangle \end{aligned}$$

where we used commutators (anticommutators) for the retarded and advanced bath (system) Green's functions. The starting point is the Dyson's equation (22). In order to obtain from the Dyson's equation (22) an equation for the lesser and greater Green's function we use the Keldysh book-keeping for a generic convolution $C(t_1, t_2) \doteq \int_\gamma d\bar{t} A(t_1, \bar{t}) B(\bar{t}, t_2)$ is $C^{r(a)}(t_1, t_2) = \int_0^t d\bar{t} A^{r(a)}(t_1, \bar{t}) B^{r(a)}(\bar{t}, t_2)$ and $C^{(< >)}(t_1, t_2) = \int_0^t dt_1 A^r(t_1, \bar{t}) B^{(< >)}(\bar{t}, t_2) + A^{(< >)}(t_1, \bar{t}) B^a(\bar{t}, t_2)$ ⁴². Using the previous formulas we rewrite the Dyson's

equations as:

$$i\partial_{t_1} G_k^<(t_1, t_2) = \mathcal{H}_k(t_1)G_k(t_1, t_2) + \int_0^t d\bar{t} \Sigma_k^r(t_1, \bar{t})G_k^<(\bar{t}, t_2) + \Sigma_k^<(t_1, \bar{t})G_k^a(\bar{t}, t_2) \quad (43)$$

and an analogous equation for ∂_{t_2} . We are interested in the *equal-time* Green's function and hence we perform a change of variables:

$$t = \frac{t_1 + t_2}{2} \\ \delta t = t_1 - t_2$$

whose Jacobian is simply $\partial_t = \partial_{t_1} + \partial_{t_2}$ and $\partial_{\delta t} = \frac{1}{2}(\partial_{t_1} - \partial_{t_2})$. At equal time ($\delta t = 0$), for the lesser Green's function $G_k^< = G_k^<(t_1, t_1) = G_k^<(t)$ we get:

$$i\partial_t G_k^< = [\mathcal{H}_k(t), G_k^<] + \Sigma_k^r \cdot G_k^< + \Sigma_k^< \cdot G_k^a - G_k^r \cdot \Sigma_k^< - G_k^< \cdot \Sigma_k^a \quad (44)$$

where the dot indicates the convolution $\Sigma_k^r \cdot G_k^< \doteq \int_0^t d\bar{t} \Sigma_k^r(t, \bar{t})G_k^<(\bar{t}, t)$. Now we use the relations:

$$G^r(t_1, t_2) = \theta(t_1 - t_2) (G^>(t_1, t_2) - G^<(t_1, t_2)) \\ G^a(t_1, t_2) = \theta(t_2 - t_1) (G^<(t_1, t_2) - G^>(t_1, t_2))$$

and similar relations that hold also for the $\Sigma^{r,a}$ (see⁴²):

$$\Sigma^{r(a)}(t_1, t_2) = \Sigma^\delta \delta(t_1, t_2) + \theta(t_{1(2)} - t_{2(1)}) (\Sigma^{>(<)}(t_1, t_2) - \Sigma^{<(>)}(t_1, t_2))$$

where we can neglect the term Σ^δ that only renormalizes the Hamiltonian and is not relevant in our case (see Eq. (48) below). At equal times we get:

$$i\partial_t G_k^< = [\mathcal{H}_k, G_k^<] + \Sigma_k^> \cdot G_k^< - \Sigma_k^< \cdot G_k^> + G_k^< \cdot \Sigma_k^> - G_k^> \cdot \Sigma_k^<$$

We now perform a Markov approximation. This will transform the integro-differential kinetic equation into a differential equation. Let us define the interaction picture for a general function:

$$\tilde{O}_k(t_1, t_2) \doteq \mathcal{U}_k^\dagger(t_1) O_k(t_1, t_2) \mathcal{U}_k(t_2)$$

where \mathcal{U}_k is the *free* evolution matrix for the system obeying $i\mathcal{U}_k = \mathcal{H}_k \mathcal{U}_k$. Such transformation gauges away the free evolution and the new Green's function \tilde{G}_k dynamics is solely governed by the self energy:

$$i\partial_t \tilde{G}_k^< = \tilde{\Sigma}_k^> \cdot \tilde{G}_k^< - \tilde{\Sigma}_k^< \cdot \tilde{G}_k^> + \tilde{G}_k^< \cdot \tilde{\Sigma}_k^> - \tilde{G}_k^> \cdot \tilde{\Sigma}_k^<$$

Since the self-energy carries the “small” perturbative coupling parameter the evolution of \tilde{G}_k can be regarded as “slow” with respect to the time scale of the self energy, that is the same as that of the bath. In fact Σ contains the bath-correlation function $g(t_1, t_2)$ (see Eq. (48)) that is strongly peaked at $t_1 \simeq t_2$ because of the assumption of a cutoff-time for the bosonic modes (see Sec. IV). Thus we can take \tilde{G} out of the convolutions:

$$i\partial_t \tilde{G}_k^< \approx \left(\int_0^t d\bar{t} \tilde{\Sigma}_k^>(t, \bar{t}) \right) \tilde{G}_k^< - \left(\int_0^t d\bar{t} \tilde{\Sigma}_k^<(t, \bar{t}) \right) \tilde{G}_k^> + \tilde{G}_k^< \left(\int_0^t d\bar{t} \tilde{\Sigma}_k^>(\bar{t}, t) \right) - \tilde{G}_k^> \left(\int_0^t d\bar{t} \tilde{\Sigma}_k^<(\bar{t}, t) \right) \quad (45)$$

Eq. (45) is quite general and it is based solely on the assumption of Markovian baths. We now use the explicit form of the self-energy for the coupling system-bath (20) with $l = 1$, that within the self-consistent Born approximation reads:

$$\Sigma_k(t_1, t_2) = \frac{i}{N} \sum_q g_{k-q}(t_1, t_2) \tau^z G_q(t_1, t_2) \tau^z \\ = \frac{i}{N} g(t_1, t_2) \tau^z \sum_q G_q(t_1, t_2) \tau^z \quad (46)$$

where $g_q(t_1, t_2) = -i \langle \mathcal{T} X_q(t_1) X_q(t_2) \rangle$ is the non-interacting bath Keldysh Green's function that does not explicitly depend on the moment q (since all baths have the same spectral function). In Eq. (46) we neglected the polaronic shift contribution (corresponding to the tad-pole diagram, Fig. 3b)

$$\Sigma_k^\delta(t_1, t_2) = -\frac{i}{N} \delta(t_1, t_2) \tau^z \int_\gamma d\bar{t} g(t_1, \bar{t}) \sum_q \text{Tr}[\tau^z G_q(\bar{t}, \bar{t})] \quad (47)$$

In fact, being such term proportional to a $\delta(t_1, t_2)$, it has only the irrelevant effect of renormalizing the Hamiltonian (see Sec. IV). Using again the Keldysh book-keeping^{40,42}, we obtain from Eq. (46), for the lesser and greater self energy

$$\Sigma_k^<(t_1, t_2) = \frac{i}{N} g^<(t_1, t_2) \tau^z \sum_q G_q^<(t_1, t_2) \tau^z \quad (48)$$

(notice that $g^>(t_1, t_2) = -g^<(t_1, t_2)^*$). Evaluating explicitly the self-energy kernels we obtain:

$$\begin{aligned}
\int_0^t d\bar{t} \tilde{\Sigma}_k^>(t, \bar{t}) &= \frac{i}{N} \sum_q \int_0^t d\bar{t} g^>(t, \bar{t}) \mathcal{U}_k^\dagger(t) \tau^z G_q^>(t, \bar{t}) \tau^z \mathcal{U}_k(\bar{t}) \\
&= \frac{i}{N} \sum_q \int_0^t d\bar{t} g^>(t - \bar{t}) \mathcal{U}_k^\dagger(t) \tau^z \mathcal{U}_q(t) \tilde{G}_q^>(t, \bar{t}) \mathcal{U}_q^\dagger(\bar{t}) \tau^z \mathcal{U}_k(\bar{t}) \\
&\simeq \frac{i}{N} \sum_q \mathcal{U}_k^\dagger(t) \tau^z \mathcal{U}_q(t) \tilde{G}_q^>(t, t) \left(\int_0^\infty ds g^>(s) \mathcal{U}_q^\dagger(t - s) \tau^z \mathcal{U}_k(t - s) \right) \\
\\
\int_0^t d\bar{t} \tilde{\Sigma}_k^>(\bar{t}, t) &= \frac{i}{N} \sum_q \int_0^t d\bar{t} g^>(\bar{t}, t) \mathcal{U}_k^\dagger(\bar{t}) \tau^z G_q^>(\bar{t}, t) \tau^z \mathcal{U}_k(t) \\
&= \frac{i}{N} \sum_q \int_0^t d\bar{t} g^>(\bar{t} - t) \mathcal{U}_k^\dagger(\bar{t}) \tau^z \mathcal{U}_q(\bar{t}) \tilde{G}_q^>(\bar{t}, t) \mathcal{U}_q^\dagger(t) \tau^z \mathcal{U}_k(t) \\
&\simeq \frac{i}{N} \sum_q \left(\int_0^\infty ds g^>(-s) \mathcal{U}_k^\dagger(t - s) \tau^z \mathcal{U}_q(t - s) \right) \tilde{G}_q^>(t, t) \mathcal{U}_q^\dagger(t) \tau^z \mathcal{U}_k(t)
\end{aligned}$$

where \simeq refers again to the Markov approximation. For the greater kernels simply interchange “ $<$ ” with “ $>$ ”. Finally, in the Schrödinger picture, using the relation $G^> = -i\mathbf{1} + G^<$, we obtain Eq. (26).

APPENDIX A2: APPROXIMATION FOR THE KINETIC EQUATION MATRICES \hat{D}

In this appendix we comment on the validity of the approximation (31) for the matrices (27) appearing in the kinetic equation. To calculate \hat{D} exactly, we need to know the evolution operator $\hat{\mathcal{U}}_k$, solution of the differential equation $i\dot{\hat{\mathcal{U}}}_k = \hat{\mathcal{H}}_k \hat{\mathcal{U}}_k$. This can be obtained exactly by mapping the dynamics of a generic mode k into a Landau-Zener two-level system dynamics^{15,30}

$$\hat{\mathcal{H}}^{LZ} \equiv h^{LZ}(t) \hat{\tau}^z + \Delta^{LZ} \hat{\tau}^x \quad (49)$$

with $\Delta_k^{LZ} = \gamma \sin k$ and $h_k^{LZ} = -vt$ that can be obtained from (15) by a simple change of the variable t . Using the solution of the Landau-Zener problem for a quench that starts at $t = -\infty$ we have for the matrix elements of $\mathcal{U}^{LZ}(-\infty, t)$,

$$\mathcal{U}^{LZ}(-\infty, t) = \begin{pmatrix} \mathcal{U}_{11}^{LZ}(t) & -\mathcal{U}_{21}^{LZ}(t)^* \\ \mathcal{U}_{21}^{LZ}(t) & \mathcal{U}_{11}^{LZ}(t)^* \end{pmatrix}$$

the following results:

$$\begin{aligned}
\mathcal{U}_{11}^{LZ}(t) &= e^{i\frac{\pi}{4}} \exp \left\{ -\frac{\pi (\Delta^{LZ})^2}{8v} \right\} \mathcal{D}_{-p}((-1+i)\sqrt{v}t) \\
\mathcal{U}_{21}^{LZ}(t) &= \frac{\Delta^{LZ}}{\sqrt{2v}} \exp \left\{ -\frac{\pi (\Delta^{LZ})^2}{8v} \right\} \mathcal{D}_{-p-1}((-1+i)\sqrt{v}t)
\end{aligned}$$

where $p = -i(\Delta^{LZ})^2/2v$ and \mathcal{D}_p are parabolic cylinder functions. Finally the evolution operator from generic \bar{t} to t can be obtained using the simple property:

$$\begin{aligned}
\mathcal{U}^{LZ}(\bar{t}, t) &= \mathcal{U}^{LZ}(-\infty, t) \mathcal{U}^{LZ}(\bar{t}, -\infty) \\
&= \mathcal{U}^{LZ}(-\infty, t) \mathcal{U}^{LZ\dagger}(-\infty, \bar{t})
\end{aligned}$$

The second ingredient we need in order to calculate \hat{D} is the bath thermal equilibrium correlation function $g^>$. From its definition:

$$\begin{aligned}
g^>(t) &\doteq -i \langle X(t) X^\dagger(0) \rangle \\
&= -i \sum_\beta \lambda_\beta^2 \left(e^{-i\omega_\beta t} \langle b_{-\beta} b_{-\beta}^\dagger \rangle + e^{i\omega_\beta t} \langle b_\beta^\dagger b_\beta \rangle \right) \\
&= -i \int_0^\infty d\omega J(\omega) [e^{-i\omega t} (1 + n_B(\omega)) + e^{i\omega t} n_B(\omega)]
\end{aligned}$$

where $n_B \equiv 1/(e^{\omega/T} - 1)$ is the Bose function and we used the definition (19) of spectral function for the bath $J(\omega) = \sum_\beta \lambda_\beta^2 \delta(\omega - \omega_\beta)$. The correlation function can be written explicitly as:

$$\begin{aligned}
g^>(t) &= -i \int_0^\infty d\omega J(\omega) \left(\coth\left(\frac{\omega}{2T}\right) \cos(\omega\tau) - i \sin(\omega\tau) \right) \\
&= -2i\alpha T^{s+1} \Gamma(s+1) \times \\
&\quad \left(\zeta(s+1, T \frac{1 + \frac{\omega_c}{T} - i\omega_c\tau}{\omega_c}) + \zeta(s+1, T \frac{1 + i\omega_c\tau}{\omega_c}) \right)
\end{aligned}$$

where Γ is the Gamma function and $\zeta(z, u) \equiv \sum_{n=0}^\infty \frac{1}{(n+u)^z}$, $u \neq 0, -1, -2, \dots$

We are now able to calculate explicitly the matrix \hat{D} and check the validity of the approximation in (31). As stated in Sec. IV, the approximation consists in considering the instantaneous transition rates induced by the

bath, independent on the velocity of the quench. This is ultimately justified by the assumption of “fast” and memoryless Markovian baths. Hence, for slow quenches when the typical time of the quench is much larger than the typical bath time-scale we expect that the magnetic field can be regarded as not evolving for the bath. Within the approximation in Eq. (31) we can perform explicitly the integration for the matrix elements of \hat{D}_{qk} over time, giving the Laplace transform of the bath Green function. We are interested only in the real part of the latter

$$\begin{aligned} g[E] &\doteq \Re\left[\int_0^\infty i g^>(t) e^{iEt}\right] \\ &= \pi (J(E) - J(-E)) \frac{\exp(\beta E)}{\exp(\beta E) - 1} \end{aligned} \quad (50)$$

$$\hat{D}_{qk}^{approx} = \frac{1}{2} \begin{pmatrix} \cos^{++} g^{+-} + \cos^{+-} g^{++} & i(\sin^{+-} g^{-+} + \sin^{++} g^{--}) \\ -i(\sin^{+-} g^{+-} + \sin^{++} g^{++}) & \cos^{-+} g^{--} - \cos^{++} g^{-+} \end{pmatrix}. \quad (51)$$

where we defined

$$\begin{aligned} \cos^{\pm\pm} &\doteq \pm \cos \theta_k \pm \cos \theta_q \\ \sin^{\pm\pm} &\doteq \pm \sin \theta_k \pm \sin \theta_q \\ g^{\pm\pm} &\doteq g[\pm \Lambda_k \pm \Lambda_q] \end{aligned}$$

The sin and cos are geometric factors specific of the system operator that couples to the bath (in our case σ^z), while the Laplace transform of the bath $g[\cdot]$ (see 50) carries information about the relaxation rates between the different energy levels, and depends explicitly on the temperature and on the nature of the baths (i.e., its spectral function). For simplicity we consider the equal indexes \hat{D}_{kk} matrices. The same results hold also for unequal indexes since the integral of the matrix elements have the same structure in both cases. In Fig. VII we compare the matrix elements obtained using the exact evolution operator with the ones given by Eq. (51). The agreement is good, validating the approximation. Deviations appear only in the limit of fast quenches $\sqrt{v} \gg T$, and in such regime the bath has a less relevant effect on the dynamics because of the short interaction time during the quench. Besides that, deviations appear far from the critical point (corresponding to $h^{LZ} \simeq 0$), i.e., far from the most relevant part of the quench according to Secs. II and VI.

APPENDIX B: FERMI GOLDEN RULE FOR THE RELAXATION TIME

In this section we derive an expression for the critical relaxation time using the Fermi golden rule for a generic system interacting with a bosonic bath. Let us

since the imaginary part gives a renormalization contribution that is negligible in the weak coupling limit $\alpha \rightarrow 0^{44}$. In the basis of the eigenvectors of $\hat{\mathcal{H}}_k$ we obtain:

assume the system-bath interaction Hamiltonian to have the form $H_{int} = AZ$ where A and Z are system and bath operator respectively. Consider a quench of the system from zero temperature to a certain finite T . The transition rate for the process of thermalization in presence of the reservoir $\rho_B^{th} \otimes (|GS\rangle\langle GS|)_S \rightarrow \rho_B^{th} \otimes \rho_S^{th}$ (where B and S refer to system and bath, respectively) is:

$$\begin{aligned} \frac{1}{\tau} &= 2\pi \sum_{f,i,k} \delta(E_f + E_k - E_i - E_{GS}) P_B^{th}(E_i/T) \\ &\quad \times P_S^{th}(E_k/T) |\langle k, f | H_{int} | GS, i \rangle|^2 \end{aligned} \quad (52)$$

where i, f and k address the bath eigenvalues and the final state of the system respectively; $P_{S(B)}^{th}$ are thermal weights. We rewrite the δ -function as $\frac{1}{2\pi} \int_{-\infty}^{\infty} dt e^{-i(E_f - E_i)t} e^{-i(E_k - E_{GS})t}$. Summing over f and i we get the bath correlation function $z(t) = \langle Z(t)Z(0) \rangle$:

$$\frac{1}{\tau} = \sum_k \int_{-\infty}^{\infty} dt e^{-i(E_k - E_{GS})t} z(t) P_S^{th}(E_k/T) |\langle k | A | GS \rangle|^2 \quad (53)$$

The time integral gives the Fourier transform of the bath correlation function, that we parametrize as

$$z[E] = J(E) f(E/T). \quad (54)$$

For instance, for a bosonic bath with spectral function $J(E) \propto E^s$ we have

$$z[E] = \begin{cases} J(E) (1 + n_B(E/T)) & E > 0 \\ J(|E|) n_B(|E|/T) & E < 0 \end{cases}.$$

By integrating over the k -modes (setting $E_{GS} = 0$), using the critical density of states $\rho(E) \propto E^{d/z-1}$, we get:

$$\frac{1}{\tau} \propto \int dE \rho(E) z[E] P_S^{th}(E/T) |A_{GS}(E)|^2,$$

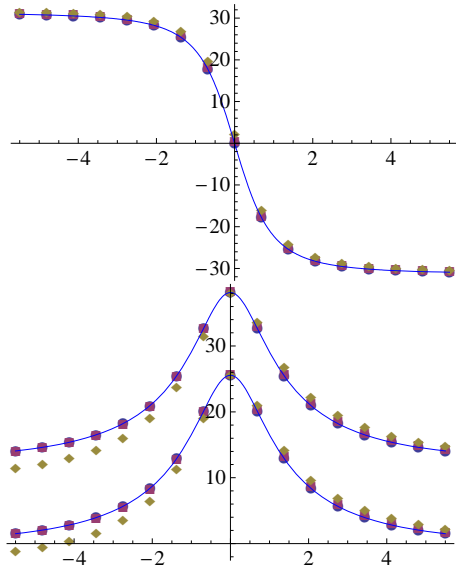


Figure 13: Matrix elements of \hat{D}_{kk} as a function of the rescaled field h^{LZ} (49); $h^{LZ} = 0$ correspond to the critical point $h \simeq 1$ for the relevant low energy modes. Lower panel: diagonal elements $i(D_{kk})_{21}$ (up) and $-i(D_{kk})_{12}$ (down); upper panel shows the difference $(D_{kk})_{11} - (D_{kk})_{22}$. Plots refer to $T/\Delta^{LZ} = 5$; continuous line is the approximation (51) (which is independent on v) and symbols are the exact value for $\sqrt{v}/T = 0.1, 1, 5$; deviations from the approximation are appreciable only for the last value of v .

where $A_{GS}(E) = \langle k(E) | A | GS \rangle$. Now, assuming that the low-energy modes (that are the relevant ones at low-temperature) are coupled uniformly by the bath $A_{GS}(E) \simeq A_{GS}(0)$ we obtain

$$\frac{1}{\tau} \propto \int dE E^{d/z-1} J(E) f(E/T) P_S^{th}(E/T) \quad (55)$$

and finally, using for the spectral density $J(E) \propto E^s$ and performing a change of variable to $x = E/T$ we obtain

$$\tau^{-1} \propto T^{s+d/z}. \quad (56)$$

-
- ¹ M. Greiner *et al.*, Nature **415**, 39 (2002); M. Greiner *et al.*, Nature **419**, 51 (2002).
² T. Kinoshita, T. Wenger, and D. S. Weiss, Nature **440**, 900 (2006).
³ L. E. Sadler *et al.*, Nature **443**, 312 (2006).
⁴ F. Iglói and H. Rieger, Phys. Rev. Lett. **85**, 3233 (2000); K. Sengupta, S. Powell, and S. Sachdev, Phys. Rev. A **69**, 053616 (2004); P. Calabrese and J. Cardy, Phys. Rev. Lett. **96**, 136801 (2006); P. Calabrese and J. Cardy, J. Stat. Mech. (2007) P10004; G. De Chiara, S. Montangero, P. Calabrese, R. Fazio, J. Stat. Mech. 0603 (2006) P001; S. Montangero *et al.*, arXiv:0810.1665v1; D. Rossini, A. Silva, G. Mussardo and G. Santoro, arXiv:0810.5508; P. Brametteler, M. Punk, V. Gritsev, E. Demler, and E. Altman, arXiv:0810.4845.
⁵ M. Rigol *et al.*, Phys. Rev. Lett. **98**, 050405 (2007); C. Kollath, A. M. Läuchli, and E. Altman, Phys. Rev. Lett. **98**, 1806012 (2007); S. R. Manmana *et al.*, Phys. Rev. Lett. **98**, 210405 (2007); M. Cramer *et al.*, Phys. Rev. Lett. **100**, 030602 (2008); T. Barthel and U. Schollwöck, Phys. Rev. Lett. **100**, 100601 (2008); M. Eckstein and M. Kollar, Phys. Rev. Lett. **100**, 120404 (2008); M. A. Cazalilla, Phys. Rev. Lett. **97**, 156403 (2006); D. M. Gangardt and M. Pustilnik, Phys. Rev. A **77**, 041604(R) (2008).
⁶ A. Polkovnikov, arXiv:0806.0620; R. Barankov and A. Polkovnikov, arXiv:0806.2862.
⁷ A. Silva, Phys. Rev. Lett. **101**, 120603 (2008); G. Roux, arXiv:0810.3720; A. Faribault, P. Calabrese, J.-S. Caux, arXiv:0812.1928.
⁸ T. W. B. Kibble, J. Phys. A **9** 1387 (1976); W. H. Zurek, Nature (London) **317** 505 (1985).
⁹ T. W. B. Kibble, Physics Today **60**, 47 (2007).
¹⁰ E. Farhi *et al.*, Science **292**, 472 (2001).
¹¹ G. E. Santoro *et al.*, Science **295**, 2427 (2002).
¹² G. E. Santoro and E. Tosatti, J. Phys. A: Math. Gen. **39**, R393 (2006).
¹³ W. H. Zurek, U. Dorner, P. Zoller, Phys. Rev. Lett. **95** 105701 (2005).
¹⁴ A. Polkovnikov, Phys. Rev. B **72**, 161201(R) (2005).
¹⁵ J. Dziarmaga, Phys. Rev. Lett. **95** 245701 (2005).
¹⁶ B. Damski, Phys. Rev. Lett. **95**, 035701 (2005).
¹⁷ R. Schützhold, M. Uhlmann, Y. Xu, and U. R. Fischer, Phys. Rev. Lett. **97**, 200601 (2006).
¹⁸ R. W. Cherng and L. S. Levitov, Phys. Rev. A, **73**, 043614 (2006).
¹⁹ B. Damski and W. H. Zurek, Phys. Rev. Lett. **99**, 130402 (2007).
²⁰ F. M. Cucchietti *et al.*, Phys. Rev. A, **75**, 023603 (2007).
²¹ L. Cincio *et al.* Phys. Rev. A, **75**, 052321 (2007).
²² T. Caneva, R. Fazio, and G. E. Santoro, Phys. Rev. B **76**, 144427 (2007).
²³ T. Caneva, R. Fazio, and G. E. Santoro, Phys. Rev. B **78**, 104426 (2008).
²⁴ K. Sengupta, D. Sen and S. Mondal, Phys. Rev. Lett. **100**, 077204 (2008).
²⁵ A. Polkovnikov and V. Gritsev, Nature Physics **4**, 477 (2008).

- ²⁶ D. Sen, K. Sengupta, and S. Mondal, Phys. Rev. Lett. **101**, 016806 (2008).
- ²⁷ U. Divakaran, V. Mukherjee, A. Dutta, D. Sen, arXiv:0807.3606v1.
- ²⁸ F. Pellegrini, S. Montangero, G. E. Santoro, R. Fazio, Phys. Rev. B **77** (2008) 140404.
- ²⁹ S. Deng, G. Ortiz, and L. Viola, arXiv:0809.2831v1.
- ³⁰ A. Fubini, G. Falci and A. Osterloh, New J. Phys. **9** 134 (2007).
- ³¹ S. Mostame, G Schaller and R. Schtzhold, Phys. Rev. A **76**, 030304(R) (2007).
- ³² M.H.S. Amin, C.J.S. Truncik and D.V. Averin, arXiv:0803.1196.
- ³³ L. Cincio, J. Dziarmaga, J. Meisner and M. M. Rams, arXiv:0812.1455v1.
- ³⁴ D. Patanè, A. Silva, L. Amico, R. Fazio, and G.E. Santoro, Phys. Rev. Lett. **101**, 175701 (2008).
- ³⁵ S. Sachdev, “*Quantum Phase Transitions*” (Cambridge University-Press, Cambridge 1999).
- ³⁶ Notice that depending on the characteristics of the bath, the system-bath coupling may lead to a change of universality class of the transition as a result of bath induced long-range correlations effects. We will not address these issues here, which deserve a careful separate study. Therefore we will assume the bath correlations to be short ranged in time³⁴.
- ³⁷ P. Pfeuty, Ann. Phys. (N.Y.), Ann. Phys. **57**, 79-90 (1970).
- ³⁸ U. Weiss, *Quantum Dissipative Systems* (World Scientific, 1992).
- ³⁹ P. Werner *et al*, Phys. Rev. Lett. **94** 047201 (2005).
- ⁴⁰ H. Haug and A.-P. Jauho, *Quantum Kinetics in Transport and Optics of Semiconductors* (Springer, Berlin, 1996).
- ⁴¹ J. Rammer and H. Smith, Rev. Mod. Phys., **58**, 323(1986).
- ⁴² R. van Leeuwen, N. E. Dahlen, G. Stefanucci, C.-O. Almbladh, U. von Barth, cond-mat/0506130.
- ⁴³ L. Landau, Physics of the Soviet Union 2: 46-51, (1932); C. Zener, Proceedings of the Royal Society of London, Series A 137 (6): 692-702, (1932).
- ⁴⁴ C. Cohen-Tannoudji, J. Dupont-Roc, G. Grynberg, *Atom-photon interactions: Basic processes and applications* (Wiley-Hermann, New-York).